Digital filter for hot-wire measurements of small-scale turbulence properties

2011 Meas. Sci. Technol. 22 125401

(http://iopscience.iop.org/0957-0233/22/12/125401)

Meas. Sci. Technol. **22** (2011) 125401 (10pp) doi:10.1088/0957-0233/22/12/125401

Digital filter for hot-wire measurements of small-scale turbulence properties

J Mi[1,2,3], M Xu[2] and C Du[2]

[1] State Key Laboratory of Turbulence and Complex Systems, College of Engineering, Peking University, Beijing 100871, People's Republic of China
[2] Department of Energy and Resources Engineering, College of Engineering, Peking University, Beijing 100871, People's Republic of China

E-mail: jcmi@coe.pku.edu.cn

Received 15 April 2011, in final form 9 September 2011
Published 19 October 2011
Online at stacks.iop.org/MST/22/125401

Abstract
The experimental work on fine-scale properties of turbulence has so far been based mainly on hot-wire and cold-wire measurements. These measurements often suffer from contamination by electronic (including thermal, shot, flicker, burst, etc) noise or from over-filtering by somewhat arbitrary, inappropriate filter settings. This may be overcome by a fast-convergent iterative scheme of filtration developed recently by Mi *et al* (2005 *Phys. Rev.* E **71** 066304). The present study is carried out (1) to investigate the effectiveness of the scheme using velocity signals (u_m) obtained from hot-wire measurements in both circular and plane turbulent jets and (2) to assess the effect of the low-pass-filter cut-off frequency on measurements of various small-scale turbulence properties. The results reveal that the electronic noise in u_m, if not cleaned, may seriously contaminate the fine-scale properties of turbulence derived from u_m, consequently yielding wrong estimations of typical scales, such as Kolmogorov and Taylor scales. After removing the noise contribution properly, however, these characteristic scales are all obtained appropriately and follow closely their self-preserving relations which have been well confirmed in the past.

Keywords: fine-scale turbulence, digital filter, high-frequency noise

(Some figures in this article are in colour only in the electronic version)

1. Introduction

Previous experimental research into fine-scale turbulence has been based predominantly on hot-wire (velocity) and cold-wire (temperature) measurements (e.g. [1]), with some on imaging measurements (e.g. [2, 3]). The skill of appropriately filtering those measured signals is thus believed to be crucial for the development of knowledge on fine-scale turbulence. While conventional methods to optimize electronic filter settings to avoid under- or over-filtering the measured signals may be devised (e.g. [4–7]), they are either cumbersome or somewhat arbitrary. It is hence believed that pure signals of fluctuating velocity, free from noise contamination, have never been obtained by hot-wire measurements. In other words, those measured velocity signals reported in the literature should always be noise-erred or over-filtered (e.g. [7]), due to the reasons detailed below. Such an unresolved problem of hot-wire measurements may be addressed partly by the scheme of Mi *et al* [8]. The present study is carried out to underpin this important issue through velocity measurements in both circular and plane turbulent jets, the two flows which have been extensively investigated so far.

Although the noise contamination has a little effect on the energy spectrum of velocity or is scalar in general when there is a sufficiently high signal-to-noise ratio (SNR, i.e. the power ratio between a true signal and the background noise), it has a great impact on the dissipation spectrum at high frequencies or low wavenumbers (e.g. [8–11]). Also importantly, the gradient calculation process acts differently on high- and low-frequency components of noise, i.e. amplifying the former and repressing the latter (e.g. [11]). Thus, for the high-frequency components, a great difference occurs between the

[3] Author to whom any correspondence should be addressed.

noise-contaminated dissipation spectrum and the true one, while their low-frequency components are nearly identical. The filtering algorithm proposed by Mi *et al* [8] can filter out the high-frequency noise in velocity signals and thus make it possible to obtain the dissipation rate of turbulence kinetic energy nearly free from noise. However, it is important to note that, as revealed by Wang *et al* [11], the noise and resolution effects are coupled so that different noise levels will lead to different errors of resolution for the measured mean scalar dissipation (and so for the energy dissipation).

The fine-scale turbulence properties are associated with velocity and scalar gradient correlations. Among them is particularly the average dissipation rate of turbulence kinetic energy defined by (e.g. [12])

$$\varepsilon = \nu \left\langle \left(\frac{\partial u_i}{\partial x_j} + \frac{\partial u_j}{\partial x_i} \right) \frac{\partial u_j}{\partial x_i} \right\rangle \tag{1}$$

with standard Cartesian tensor notation and summation on repeated indices; where i (or j) = 1, 2 and 3 represent the streamwise, lateral and spanwise directions, respectively. The reference scales for the fine-scale turbulence are often the Kolmogorov length scale

$$\eta \equiv \left(\frac{\nu^3}{\varepsilon} \right)^{1/4} \tag{2}$$

and also the Kolmogorov frequency scale

$$f_K \equiv \frac{U}{2\pi\eta}, \tag{3}$$

where ν is the kinematic viscosity and U is the local mean velocity. However, there is a key question arising here: how can we accurately estimate these scales from the velocity measurement?

Raw or non-filtered signals of measured velocity, u_{im} (the subscript 'm' means 'measured'), are inevitably contaminated by electronic noise (n), namely

$$u_{im} = u_i + n. \tag{4}$$

This contamination causes both the spatial and temporal gradient variances to be overestimated, i.e.

$$\left\langle \left(\frac{\partial u_{im}}{\partial x_j} \right)^2 \right\rangle = \left\langle \left(\frac{\partial u_i}{\partial x_j} \right)^2 \right\rangle + \left\langle \left(\frac{\partial n}{\partial x_j} \right)^2 \right\rangle \tag{5}$$

and

$$\left\langle \left(\frac{\partial u_{im}}{\partial t} \right)^2 \right\rangle = \left\langle \left(\frac{\partial u_i}{\partial t} \right)^2 \right\rangle + \left\langle \left(\frac{\partial n}{\partial t} \right)^2 \right\rangle, \tag{6}$$

where $i = 1, 2$ or 3 but $j = 2$ or 3 (note: a multi-hot-wire probe is unable to measure the streamwise derivatives $\partial u_i/\partial x_1$ due to the downstream wire being located in the thermal wake of the upstream wire). The terms $\langle(\partial n/\partial x_j)^2\rangle$ and $\langle(\partial n/\partial t)^2\rangle$ are redundant from noise. Accurate measurements require that u_{im} be low-pass filtered at a specific cut-off frequency f_c to eliminate the effect of high-frequency ($\geqslant f_c$) electronic noises. The selection of f_c is vital: too high a value will not clean high-frequency noises sufficiently, while too low a value will remove some of the true signals. The use of $f_c = f_K$ should be the right choice (e.g. [13, 14]). However, f_K is not only a function of the flow but also varies spatially in almost any flow. That is, it cannot be determined *a priori*, although its determination was claimed by all previous studies with hot-wire measurements (e.g. [4, 13–15]). The hardware method used by Antonia *et al* [15] or others to determine f_c on-site for hot-wire measurements of any fine-scale properties of turbulence is complex, requiring two electronic analog filters, a differentiator, a real-time spectrum analyzer, visual inspection and optimization ideally at *each* measurement location. This procedure of hot-wire measurements is only realistic where the number of data points is limited and is prohibitive for experiments requiring a large number of spatial locations or flow conditions. In the absence of a simpler procedure, more arbitrary criteria are usually adopted, so that most previous hot-wire measurements of ε must be contaminated by noise to some extent. The importance of this issue is also deduced from Mi and Nathan [10] who showed that even slightly over-filtering u_{im} at $f_c < f_K$ may cause substantial underestimation of the velocity gradients. The development of the iteratively filtering scheme by Mi *et al* [8] appears to have resolved the problem for hot-wire measurements. This digital scheme described in the next section can more appropriately obtain f_K without prior knowledge of η.

The present study is carried out to systematically examine the scheme using the data obtained in both circular and plane turbulent jets. The objective is threefold.

(1) To reinforce the validity of the scheme, if valid, through the estimation of various characteristic scales of turbulence.
(2) To assess the effect of filter on the hot-wire measurements of various turbulence properties.
(3) To investigate, based on 'cleaned' data, the centerline evolutions of the mean and RMS velocities, the dissipation rate of turbulence kinetic energy, and the Kolmogorov and Taylor micro-scales.

Measurements are performed using hot-wire anemometry at the exit Reynolds number approximately of 20 000 and 9000, respectively, for the circular and plane jets.

2. Digital scheme of filtration by Mi *et al* [8]

Suppose that the measured dissipation rate ε_m is expressed as

$$\varepsilon_m = \varepsilon[\text{true dissipation}] + \varepsilon_n[\text{noise contribution}] = C\varepsilon \tag{7}$$

with $C = (1 + \varepsilon_n/\varepsilon) > 1$ when filtration is insufficient or $C < 1$ if over-filtering. Substituting (7) into (2) leads to

$$\eta_m = (\nu^3/C\varepsilon)^{1/4} = C^{-1/4}\eta. \tag{8}$$

It is then obtained from equation (3) that

$$f_{Km} = C^{1/4} f_K. \tag{9}$$

Based on (7)–(9) for the case $C = (1 + \varepsilon_n/\varepsilon) > 1$, Mi *et al* [8] have proposed an iterative scheme to obtain the 'true' values of η and f_K from the post-processing of the sampled signals of u_{im} and simultaneously to 'clean' u_{im} properly. *The scheme uses* (7)–(9) *circularly to 'squeeze out' the noise-contribution from* u_{im} *by filtering* u_{im} *at new* f_{Km} *iteratively.* The principle is based on the fact that the noise imposes a significantly greater influence on ε_m than on both η_m and f_{Km}. For instance, when

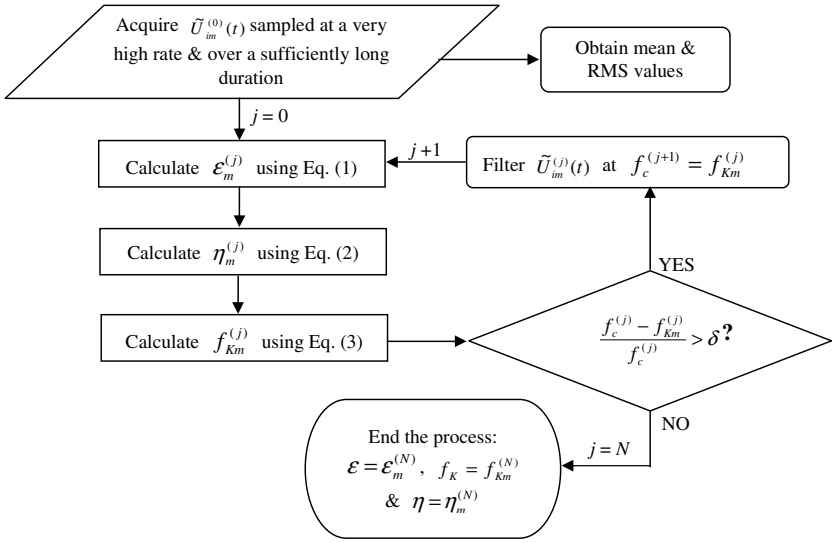

Figure 1. Iterative scheme of the digital filter (reproduced from Mi *et al* [8]).

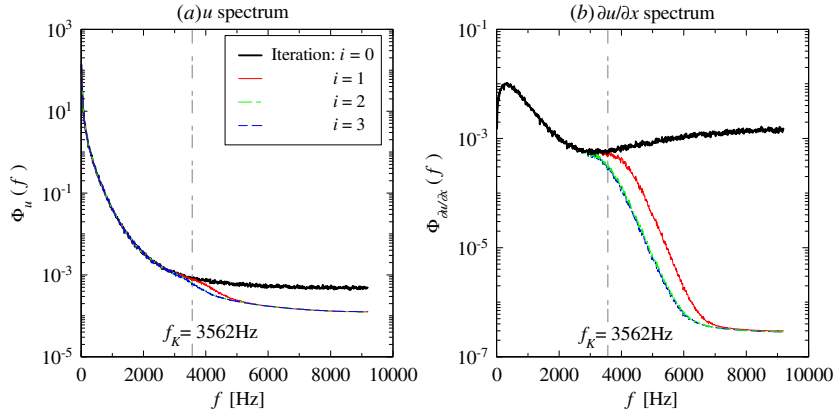

Figure 2. Centerline spectra of the original and filtered signals of (a) the streamwise velocity u_m and (b) its derivative $\partial u_m/\partial x$ obtained at $x/d = 30$ in a circular jet.

$\varepsilon_m = 5\varepsilon$, the resulting values of η_m and f_{Km} are $\eta_m = 0.67\eta$ and $f_{Km} = 1.5 f_K$.

Figure 1 shows a flow chart of the scheme, reproduced from Mi *et al* [8]. With the measured $u_{im}^{(0)}$, calculations of $\varepsilon_m^{(0)}$, $\eta_m^{(0)}$ and $f_{Km}^{(0)}$ can be made from equations (1)–(3). If $\left(f_c^{(0)} - f_{Km}^{(0)}\right)/f_c^{(0)} > \delta$ (e.g. taking $\delta = 10^{-4}$), where $f_c^{(0)} = \infty$ if originally no filtering, the action of digitally filtering $u_{im}^{(0)}$ at $f_c^{(1)} = f_{Km}^{(0)}$ is taken, generating the new signal $u_{im}^{(1)}$. The above process may be repeated until $\left(f_c^{(N)} - f_{Km}^{(N)}\right)/f_c^{(N)} \leqslant \delta$ or $f_{Km}^{(N)}$, $\eta_m^{(N)}$ and $\varepsilon_m^{(N)}$ have converged to their 'true' values, i.e. $\varepsilon = \varepsilon_m^{(N)}$, $f_K = f_{Km}^{(N)}$ and $\eta = \eta_m^{(N)}$.

The applicability of the filtering algorithm has been tested at various SNRs of the time gradient of the streamwise velocity ($\partial u_m/\partial t$; hereafter the subscript '1' for the streamwise direction is omitted for simplification, i.e. $x \equiv x_1$, $u_m \equiv u_{1m}$ and $u \equiv u_1$) introduced artificially or obtained at largely different locations in flow (e.g. SNR decreases significantly with downstream or radial distance in jet flows). It is revealed that the scheme works well for all the tested SNRs even down to SNR = 0.1. Figure 2 shows an example for SNR $\approx$ 1.72. It presents the one-dimensional spectra, at different iterations of filtering, of the streamwise fluctuating velocity u_m and its derivative $\partial u_m/\partial t$ obtained on the centerline at $x/d = 30$ in the circular jet of present investigation (see section 3 for more details). The high-frequency noise is reduced drastically at the first iteration. Then, the spectra converge rapidly to their 'true' values in the next two to three iterations. This can also be seen clearly from the variations of the measured Kolmogorov and cut-off frequencies, i.e. $f_{Km}^{(i)}$ and $f_c^{(i)} = f_{Km}^{(i-1)}$ (see figure 3). The convergent Kolmogorov frequency is $f_K \approx$ 3562 Hz and the convergent ratios $(\langle u_m^2\rangle - \langle u^2\rangle)/\langle u^2\rangle$ and $(\varepsilon_m - \varepsilon)/\varepsilon$ are approximately 0.6% and 58% (i.e. SNR $\approx$ 1.72).

Note that the present study employs the fifth-order Butterworth low-pass filter, widely used in the literature, for application of the scheme. Nevertheless, tests of the third-, fifth-, seventh-order Butterworth low-pass filters and the tenth-order Chebyshev low-pass filter show no dependence of the scheme on the filter type. It should be indicated as well that both $f_{Km}^{(j)}$ and $\eta_m^{(j)}$ can generally converge to their 'asymptotic'

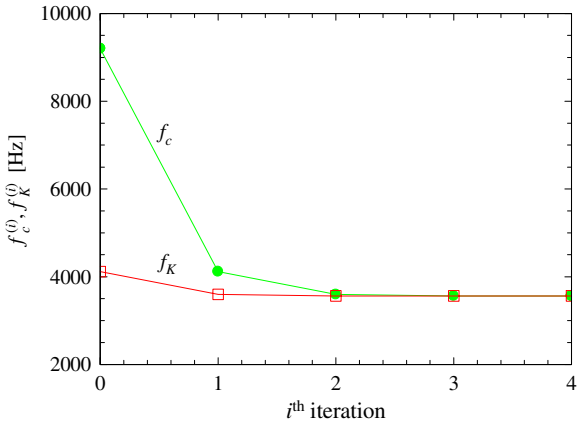

Figure 3. Variations of the measured cut-off and Kolmogorov frequencies at different iterations for the circular jet at $x/d = 30$.

values at the fourth iterations when $\delta = 10^{-4}$. Besides, if the analog filter is needed for the removal of the aliasing effects, the application of the scheme will require that the electronic cut-off frequency be $f_c \geqslant f_{Km}^{(0)} = U_{1m}^{(0)}(2\pi)^{-1}(\varepsilon_m^{(0)}/\nu^3)^{1/4}$ and thus that the sampling rate is taken to be $f_s \geqslant 2f_c$; otherwise, we suggest that $f_s \geqslant 2f_{Km}^{(0)}$. In addition, a sufficiently long sampling duration (e.g. 60 s) should be taken for good statistical data.

For convenience, in the following, ε_m, η_m and f_{Km} represent the original values (i.e. $j = 0$) and the convergence results (i.e. $j = N$) are represented by ε, η and f_K.

3. Experimental description

It is well known that a great difficulty occurs in directly measuring ε and so in the related quantities (η, f_K). The direct measurement of ε requires direct measurements of all gradient correlations in (1). Further, the accurate measurement of any component of ε requires a multi-sensor probe with exceptionally high spatial and temporal resolutions to 'feel' the finest-scale or most-rapid velocity fluctuations. All these, however, cannot be realized by experimental techniques available currently and in foreseeable future. Hence, to validate the digital filter in turbulent flows, this study has to estimate ε, like most of the previous work, from hot-wire measurements of the streamwise instantaneous velocity (u_m) using the isotropic relation $\varepsilon = 15\nu\langle(\partial u/\partial x)^2\rangle$ together with Taylor's hypothesis (see section 4.1).

The centerline measurements of u_m using hot-wire anemometry are made in a circular jet and also a plane jet. Here only a brief description for each jet facility is given below as their details may be found elsewhere (e.g. [16, 17]).

(a) *Circular jet*: The present jet facility consists of a cylindrical plenum chamber with an internal diameter of 95 mm and a length of 600 mm. Filtered and compressed air is supplied through the plenum to a smooth contraction nozzle, flush with a flat surface of 200 mm in diameter; see more details in [17]. The nozzle outlet profile is third-polynomial, contracting from a diameter of 95 mm to the exit diameter of $d = 20$ mm. This enables the exit profile of the mean velocity to be 'top-hat'-shaped, i.e. uniform except from near the inner wall. The exit velocity is $U_j \approx 14.9$ m s^{-1} and the corresponding Reynolds number $\mathrm{Re}(\equiv U_j d/\nu)$ is approximately 20 100. The measurements are made along the centerline at $x/d \leqslant 30$, where x is the downstream distance measured from the nozzle exit.

(b) *Plane jet*: The jet issues from a rectangular ($w \times d = 720$ mm $\times$ 20 mm) slot, with aspect ratio $w/d = 36$ (note: d represents the height or short side of the rectangular slot for the plane jet). The inner wall of each side of the slot is radially rounded with a radius of $r = 36$ mm (thus $r/d = 1.8$) to achieve a 'top-hat' velocity profile at the exit (see [16]). To ensure a two-dimensional flow, two parallel plates (2000 mm $\times$ 1800 mm) are attached to the short sides of the slot so that the jet can entrain the ambient only in the lateral direction. The jet exit velocity is $U_j \approx 6.7$ m s^{-1}, which corresponds to a Reynolds number of $\mathrm{Re} \approx 9125$. Velocity measurements are performed over the region $x/d \leqslant 40$.

All the above measurements are made using a single hot-wire (tungsten) probe, operated by an in-house constant temperature circuit with an overheat ratio of 1.6. The hot-wire sensor, aligned perpendicular to the streamwise direction, is selected to be 5 μm in diameter (d_w) and 1.0 mm in length (l_w) so that $l_w/d_w \approx 200$. It is normally suggested that $l_w/d_w \geqslant 200$, according to Hinze [12] and Champagne *et al* [18]. For the present experimental conditions, the frequency response of the hot wire and anemometer, determined by the square-wave technique, is about 100 kHz, so that the temporal resolution of the wire is approximately 10^{-5} s. To avoid aerodynamic interference of the prongs on the hot wire, the probe is carefully mounted, with prongs parallel to the jet exit. Hot-wire calibrations are conducted using a standard static Pitot tube located side by side with the probe in the jet's potential core where the velocity field is quite uniform with the turbulence intensity of about 0.5% for both jets. The calibration data are fitted using the third polynomial. To achieve the possible maximum SNR, the voltage signals from the wire are offset and amplified through the circuits. All hot-wire signals taken are low-pass filtered with an identical cut-off frequency of $f_o = 9.2$ kHz, the maximum value set by the anemometer, to eliminate excessively high-frequency noise and also to avoid any aliasing. Then they are digitized at $f_s = 18.4$ kHz via a 12 bit A/D converter on a personal computer. The sampling duration is approximately 30 s for the circular jet and 22 s for the plane jet.

4. Data processing method and assessment

4.1. Use of Taylor's hypothesis

This study has to convert time derivatives into streamwise derivatives using Taylor's hypothesis, namely

$$\langle(\partial/\partial x)^2\rangle = U^{-2}\langle(\partial/\partial t)^2\rangle, \tag{10}$$

where U is the local mean velocity. Based on the work of Mi and Antonia [19], the resulting data are not corrected for

the high turbulence intensity effect, although $\langle u^2\rangle/U \geqslant 20\%$ at $x/d > 10$ in both jets (see figure 4). Using a passive scalar (temperature) in a circular jet ($x/d = 30$) of $\mathrm{Re} = 1.9 \times 10^4$, Mi and Antonia [19] checked the hypothesis (10) and several of its corrections such as

$$\langle(\partial/\partial x)^2\rangle = \langle(\partial/\partial t)^2\rangle[U^2 + \langle u^2\rangle + \langle v^2\rangle + \langle w^2\rangle]^{-1} \quad (11)$$

proposed by other investigators (e.g. [20, 21]) for the effect of high turbulence intensity. These authors found that equation (11) is closely satisfied in the fully turbulent region across the jet. They argued that the assumptions underpinning equation (11), i.e. homogeneity and independence between small scales and large scales, are approximately satisfied in that flow region. Very important for this study, they revealed that the departure from local isotropy, in terms of the mean square scalar derivatives, is small along the jet centerline, thus suggesting the applicability of $\varepsilon = 15\nu\langle(\partial u/\partial x)^2\rangle$. Because of this, equation (10) performs well on the jet axis, even without taking any correction for high values of $\langle u^2\rangle/U_c$ and $\langle v^2\rangle/U_c$.

4.2. Data processing algorithm

The centerline velocity measurements by hot-wire anemometry described in section 3 yield the original streamwise velocity signals $\tilde{U}_m(t) = U_m + u_m(t)$ and, consequently, the original time derivative:

$$\frac{\partial u_m}{\partial t} \approx \frac{\Delta u_m}{\Delta t} = \left[u_m\left(t + f_s^{-1}\right) - u_m(t)\right] f_s. \quad (12)$$

It follows that the measured dissipation, estimated from the assumption of isotropic turbulence and Taylor's hypothesis, can be expressed plausibly by

$$\varepsilon_m \approx 15\nu U_m^2\langle(\partial u_m/\partial t)^2\rangle \approx 15\nu U_m^2 f_s^2\langle(\Delta u_m)^2\rangle. \quad (13)$$

Equations (12) correspond to the first-order two-point backward difference stencil used in numerical simulations. Wang *et al* [11] have found that it obtains less accurate estimation of the scalar dissipation rate than the use of high-order spectral-like stencils. Note that the latter are developed by Lele [22] for evaluating the scalar derivatives in computational fluid dynamics. Thus, to calculate the derivative more accurately, the present study also adopts the latter algorithm to calculate the velocity gradient and thus the dissipation rate. These stencils may be expressed as

$$\begin{aligned}&\beta g(i-2) + \alpha g(i-1) + g(i) + \alpha g(i+1) + \beta g(i+2)\\ &= c\frac{u_m(i+3) - u_m(i-3)}{6\Delta t} + b\frac{u_m(i+2) - u_m(i-2)}{4\Delta t}\\ &\quad + a\frac{u_m(i+1) - u_m(i-1)}{2\Delta t},\end{aligned} \quad (14)$$

where the parameters α, β, a, b and c are determined by substituting Taylor series expansion confidents and g represents the implicitly determined local derivative of u_m. The fourth-order seven-point scheme has been found by Wang *et al* [11] to be the best for the estimation of the dissipation whose parameters are $\alpha = 0.577\,1439$, $\beta = 0.089\,6406$, $a = 1.302\,5166$, $b = 0.993\,5500$ and $c = 0.037\,502\,45$.

4.3. Hot-wire resolution analysis

The response frequency ($\approx 10^5$ Hz) of the hot wire producing $u_m(t)$ is much higher than the sampling frequency of $u_m(t)$, i.e. $f_s = 18\,400$ Hz. Namely the temporal difference of ${f_s}^{-1}$ used for the calculation of ε_m is well within the temporal resolution of the hot wire. When the operation of filtering $u_m(t)$ is taken, the spatial difference (Δx) converted by Taylor's hypothesis from $\Delta t = {f_s}^{-1}$ varies from 0.13 mm ($x/d = 10$) to 0.06 mm ($x/d = 40$) for the plane jet and from 0.14 mm ($x/d = 19$) to 0.08 mm ($x/d = 33$) for the circular jet. By comparison, the corresponding value of the Kolmogorov scale is estimated to be $\eta \approx 0.12$ ($x/d = 10$) to 0.21 mm ($x/d = 40$) for the plane jet and $\eta \approx 0.13$ ($x/d = 19$) to 0.20 mm ($x/d = 33$) for the circular jet. Accordingly, the 'spatial' resolution converted from $\Delta t = {f_s}^{-1}$ for use of Taylor's hypothesis is appropriate to resolve the smallest scales at $x/d \geqslant 10$ for the plane jet and at $x/d \geqslant 19$ for the circular jet, where the digital filter is used for this study.

In contrast, the spatial resolution of the 1 mm hot wire is not as good, considering that $l_w/\eta = 5$–10 over these flow regions. This length however has to be chosen for $d_w = 5\ \mu$m since the ratio $l_w/d_w \geqslant 200$ is generally needed for a proper hot-wire probe with a nearly uniform temperature distribution in its central portion and high sensitivity [12, 18]. (Undoubtedly, the same issue has been involved in most, if not all, of the previous studies experimentally using hot-wire anemometry, despite its negligible effect on the mean velocity and RMS measurements.) On the other hand, unlike the measured fluctuating velocity u_m and especially its derivatives, see equations (5) and (6), the effect of electronic noise ($\partial n/\partial t$) on the temporal derivatives $\partial u_{im}/\partial t$ ($i = 1, 2, 3$) or the streamwise ones $\partial u_{im}/\partial x$, from Taylor's hypothesis, is virtually uncorrelated with the hot-wire length and even the measurement location in the flow field; see equation (6). That is, if no filter acts, the noise effect should always exist at a similar level, no matter how small or big the ratio l_w/d_w is. It is hence expected that the hot-wire length should not be critical for the present study.

5. Results and discussion

5.1. Mean and RMS velocities

To check the influence of noise on the mean and RMS velocities, the centerline results of U_m/U_j and $\langle u_m^2\rangle^{1/2}/U_m$ for the two jets are presented in figures 4(a) and (b), respectively. Figure 4(a) clearly suggests that U_m/U_j for both jets at $x/d \geqslant 8$ follows closely the relations for self-preservation of the mean velocity, i.e.

$$(U_c/U_j)^\alpha = K_U[(x - x_o)/d]^{-1} \quad (15)$$

with $\alpha = 1$ and 2 for the circular jet and plane jet, where U_c denotes the centerline true mean velocity. The centerline distribution of $\langle u_m^2\rangle^{1/2}/U_m$ is not as good but tends to approximately satisfy that

$$\langle u^2\rangle^{1/2}/U_c = K_u \quad (16)$$

at $x/d \geqslant 18$ for the two flows. Both K_U and K_u from (15) and (16) are constants determined by experiment. Note

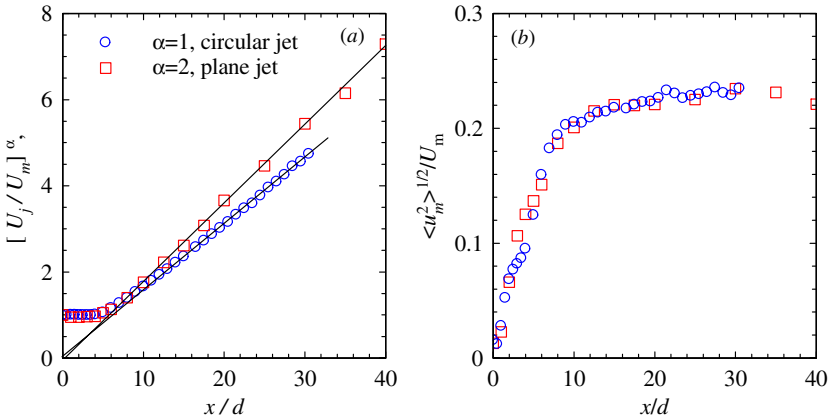

Figure 4. Centerline distributions of (*a*) normalized mean and (*b*) RMS velocities.

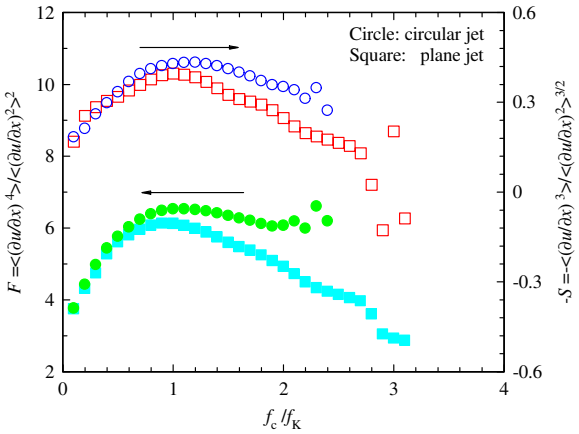

Figure 5. Skewness and flatness factors of $\partial u/\partial x$ as functions of cut-off frequency f_c for both circular and plane jets at $x/d = 30$.

that equation (16) is required for the self-preservation of the fluctuating field in both jets. It is hence suggested that $U_m \approx U_c$ and $\langle u_m^2 \rangle \approx \langle u^2 \rangle$. That is, the measured noise does not really affect both the mean and RMS velocities. This is expected because $U_m = \langle U_c + u_m \rangle = U_c$ and $\langle u_m^2 \rangle = \langle u^2 \rangle + \langle n^2 \rangle \approx \langle u^2 \rangle$ since $\langle u^2 \rangle \gg \langle n^2 \rangle$; note that u and n are uncorrelated, i.e. $\langle un \rangle = 0$. As such, the velocity half-width, L, a lateral distance at which $U = 0.5U_c$, should be virtually free from the noise contamination. Indeed, it is well confirmed that the measured results of L in the far field of each jet are consistent with the self-preserving relation

$$L/d = K_L(x - x_o)/d \tag{17}$$

with the constant K_L being determined by experiment.

5.2. Low-pass-filter cut-off frequency (f_c) versus Kolmogorov frequency (f_K)

Figure 5 shows the f_c-dependence of the skewness and flatness factors of $\partial u/\partial x$, i.e. $S \equiv \langle(\partial u/\partial x)^3\rangle/\langle(\partial u/\partial x)^2\rangle^{3/2}$ and $F \equiv \langle(\partial u/\partial x)^4\rangle/\langle(\partial u/\partial x)^2\rangle^2$, for both circular and plane jets. Since the PDF of $\partial u/\partial x$ is far from Gaussian (not presented), S and F should differ significantly from the Gaussian values (0, 3). Figure 5 clearly demonstrates that both S and F first increase with f_c before reaching their maxima (0.4–0.44; 6.1–6.5) around $f_c = f_K$ and then decrease with larger values of f_c. When $f_c \ll f_K$ or as $f_c \to 0$, the low-frequency component of $\partial u/\partial x$ should approach that of u which is near Gaussian on the centerline (not shown). As f_c increases at $f_c > f_K$, the measured $\partial u_m/\partial x$ will be increasingly contaminated by noise. Consequently, the magnitudes of S and F will drop since the random noise is often Gaussian. Similar f_c-dependences of S and F are observed by Kuo and Corrsin [13]. It is thus suggested that $f_c = f_K$ is the right choice for the low-pass-filter cut-off frequency.

However, Antonia *et al* [15] observe that the maxima of S and F are reached approximately at $f_c = 1.75{f_K}^*$. This discrepancy may be due to different methods to set the cut-off frequency. Antonia *et al* [15] obtain their 'Kolmogorov frequency' ${f_K}^*$ as follows. First, f_c is determined from $\Phi_{\partial u/\partial t}$, the spectrum of the unfiltered $\partial u/\partial t$, at which $\Phi_{\partial u/\partial t}$ exceeds its own minimum at $f_{\min}$ by 2 dB, a value somewhat arbitrarily taken. Then, ${f_K}^*$ is obtained from (3) where the dissipation ε_m is estimated from (13) using u_m filtered at $f_c < f_{\min}$. By contrast, the present f_c is determined from (7)–(9) and (13), without any arbitrariness, in the process of digitally filtering u_m (see figure 1). It might be proper to consider that the value of $1.75{f_K}^*$ obtained by Antonia *et al* [15] is the real Kolmogorov frequency, i.e. $f_K = 1.75{f_K}^*$.

5.3. Spectra of turbulence kinetic energy and dissipation

The one-dimensional spectra for $\langle u^2 \rangle$ and ε are defined as

$$\langle u^2 \rangle = \int_0^\infty \Phi_u(f)\,\mathrm{d}f \tag{18}$$

and

$$\varepsilon = \int_0^\infty \Phi_{\partial u/\partial x}(f)\,\mathrm{d}f. \tag{19}$$

To estimate the one-dimensional dissipation spectrum, it is necessary to use the assumption of local isotropy (e.g. [23]), i.e. $\varepsilon = 15\nu\langle(\partial u/\partial x)^2\rangle$. Figures 6(*a*) and (*b*) show Φ_u and $\Phi_{\partial u/\partial x}$ calculated from the centerline $u_m(t)$ and those filtered at the fourth iteration; the original data, plotted also in figure 2, were obtained on the centerline at $x/d = 30$ in the

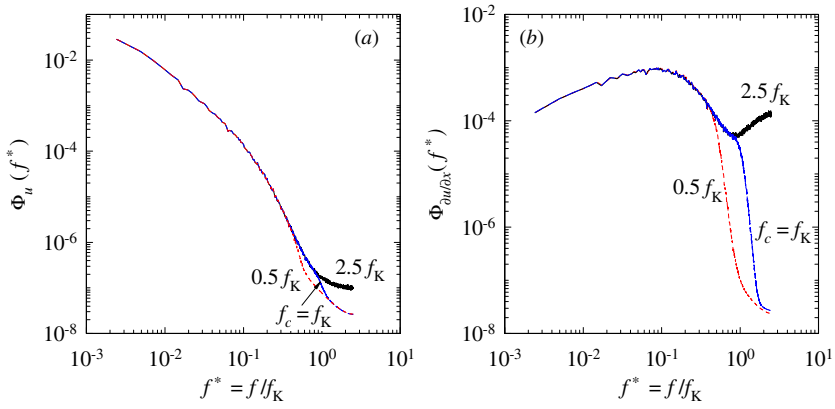

Figure 6. Spectra of the original and filtered signals of (*a*) kinetic energy and (*b*) dissipation rate at $x/d = 30$.

circular jet, where the convergent $f_K = 3562$ Hz. It is seen that the contributions of the 'noise' to $\langle u_m^2 \rangle$ and to ε_m are very different. The ratios $(\langle u_m^2 \rangle - \langle u^2 \rangle)/\langle u^2 \rangle$ and $(\varepsilon_m - \varepsilon)/\varepsilon$, for example, are estimated to be approximately 0.3% and 56% for $f_c = 2.5 f_K$ in the circular jet, while these ratios are 0.6% and 468% for $f_c = 4.1 f_K$ at $x/d = 40$ on the plane jet centerline (the spectra are not presented). That is, the high-frequency noise contamination, if not properly filtered out, has a great impact on ε_m, while its influence on $\langle u_m^2 \rangle$, or $\langle u_{im}^2 \rangle$, in a more general sense, is much less. When considering the case of over-filtering $u_m(t)$ for the circular jet, the two ratios of about -0.01% and -11% are obtained for $f_c = 0.5 f_K$, suggesting the influence of over-filtering to be very small on $\langle u_m^2 \rangle$ but significant on ε_m. Accordingly, these results together imply that, while large-scale (low-frequency) turbulent motions control the magnitude of $\langle u_i^2 \rangle$, the small-scale (high-frequency) fluctuations of velocity contribute predominantly to ε.

5.4. Dissipation rate and characteristic scales of turbulence

For turbulent flows of a sufficiently high Reynolds number, it is usually considered that ε is equal to the supply rate of the turbulence kinetic energy from the large-scale structures, which is of order U_0^3/L_0 (here U_0 and L_0 are the local characteristic velocity and length scales), (see, e.g., [24–26]). Based on this argument, we obtain that

$$\varepsilon = K_\varepsilon U_c^3 / L \tag{20}$$

when taking $U_0 = U_c$ and $L_0 = L$ for both jets, where K_ε is a constant determined by equation (20). It follows from (15)–(17) and (20) that self-preservation of the turbulent jet requires

$$\varepsilon\left(U_j^{-3} d\right) = C_\varepsilon [(x - x_0)/d]^{-(3+\alpha)/\alpha} \quad \text{with} \quad C_\varepsilon = K_\varepsilon K_U^{3/\alpha} K_L^{-1} \tag{21}$$

$$\eta/d = C_\eta \mathrm{Re}^{-3/4} [(x - x_0)/d]^{(3+\alpha)/4\alpha} \quad \text{with} \quad C_\eta = C_\varepsilon^{-1/4} \tag{22}$$

$$f_K d/U_j = C_f \,\mathrm{Re}^{3/4} [(x - x_0)/d]^{-(7+\alpha)/4\alpha} \quad \text{with} \quad C_f = (2\pi)^{-1} K_U^{1/\alpha} C_\varepsilon^{1/4} \tag{23}$$

$$\lambda/d = C_\lambda \mathrm{Re}^{-1/2} [(x - x_0)/d]^{(\alpha+1)/2\alpha} \quad \text{with} \quad C_\lambda = \sqrt{15} K_u K_U^{1/\alpha} C_\varepsilon^{-1/2} \tag{24}$$

$$\mathrm{Re}_\lambda = C_R \,\mathrm{Re}^{1/2} [(x - x_0)/d]^{(\alpha-1)/2\alpha} \quad \text{with} \quad C_R = \sqrt{15} K_u^2 K_U^{2/\alpha} C_\varepsilon^{-1/2}, \tag{25}$$

where $\alpha = 1$ and 2, respectively, for the circular and plane jets. In (24), λ denotes the Taylor microscale defined by $\lambda \equiv \langle u^2 \rangle^{1/2} \langle (\partial u/\partial x)^2 \rangle^{-1/2}$, whereas in (25), Re_λ is the turbulence Reynolds number obtained by $\mathrm{Re}_\lambda = \langle u^2 \rangle^{1/2} \lambda/\nu$. Here it should be pointed out that the constants C_ε, C_η, C_f, C_λ and C_R may be determined by fitting measured data to (21)–(25) or by the constants K_U, K_u, K_L and K_ε obtained from the measurements of the mean velocity and the centerline RMS velocity through equations (15)–(17) and (20). Note also that, if not considering the effects of using Taylor's hypothesis and isotropic turbulence assumption, the measurement uncertainties in K_U, K_u, K_L and K_ε are estimated to be approximately 0.6%, 2.0%, 1.0% and 3.5% which are converted to 6.0%, 2.6%, 2.8%, 4.2% and 6.5% for those of C_ε, C_η, C_f, C_λ and C_R. Nevertheless, these measurement errors should not be vital for the verification of the digital iterative filter.

Previous work such as Antonia *et al* [4] has proven most of (21)–(25) by experiments. For this reason, we make use of these relations to check the filtering scheme of Mi *et al* [8] below.

As justified early in section 5.2, the right choice of the cut-off frequency is $f_c = f_K$. Practices reveal that, when taking $\delta = 10^{-4}$ (see figure 1), the scheme of Mi *et al* [8] only requires four iterations for all the present turbulence statistics to converge to their 'true' values. Important to note, the original cut-off frequency $f_o = 9.2$ kHz is not high enough for the near-field measurements in both jets. In fact, f_{Km} (thus f_K) is greater than f_o over the region $x/d < 10$ for the plane jet and $x/d < 19$ for the circular jet. That is, $f_c < f_K$ or the over-filtering of u_m has occurred, so that the mean dissipation rate is underestimated, in the near fields of the jets. Accordingly, the operation of filtering u_m is taken only at $x/d \geqslant 10$ for the plane jet and at $x/d \geqslant 19$ for the circular jet. Figure 7 presents the convergent result of Kolmogorov frequency (f_K) by open

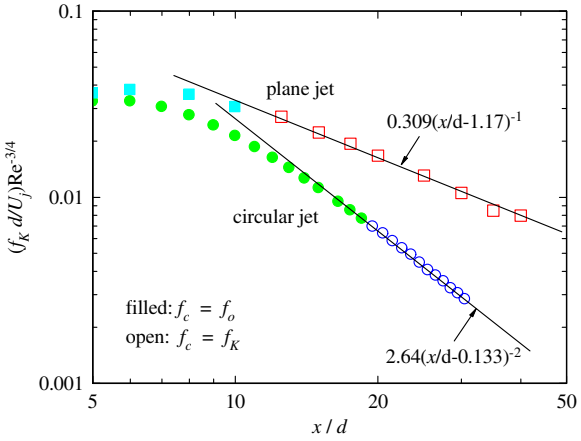

Figure 7. Measured Kolmogorov frequency along the jet centerline.

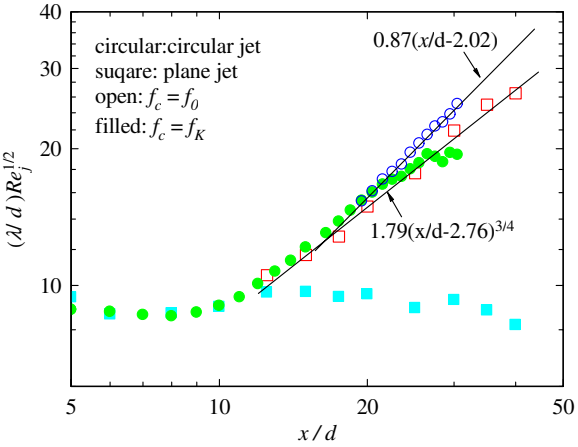

Figure 9. Centerline variation of the Taylor scale.

symbols. Obviously, equation (23), as indicated by lines, is valid over the region where the filtering operation is taken by the code, i.e. at $x/d \geqslant 19$ and 10 for the circular and the plane jet, respectively. Upstream from the region, the true f_K must be greater than f_{Km} since the latter is obtained from the over-filtered u_m or equation (9) at $C < 1$. Indeed, all the values of f_{Km} fall below the best-fit curve of f_K from equation (23) for both jets.

Figures 8 and 9 demonstrate that the data of ε, η and λ agree very well with (21), (22) and (24) at $x/d \geqslant 10$ and 19 for the plane and circular jets. This, in return, provides strong support for the validity of the iterative scheme. As x increases, f_K decreases and thus the ratio f_o/f_K increases, so that the relative contribution of electronic noise grows rapidly. Consequently, ε_m, η_m and λ_m show increased departures from their true values with increased x. That is, ε_m lies well above (21), while η_m and λ_m fall below (22) and (24), respectively.

Figures 8 and 9 also illustrate the effect of over-filtering $u_m(t)$ on ε_m, η_m and λ_m at $x/d < 10$ and 19, respectively, for the plane and circular jets. In this case, the measured values of ε_m, η_m and λ_m never agree with relations (21), (22) and (24), not only because of the over-filtering but also because self-preservation may not be satisfied in the flow region. Importantly, in the near and transition flow regions, very high low-pass filtering cut-off frequencies must be chosen since f_K is extremely high. In particular, for $x/d < 8$, the present choice of $f_o = 9.2$ kHz is relatively too low so that, as seen clearly, ε_m is significantly underestimated. Accordingly, the action of electronic filter on velocity and its gradients is not suggested, although high rapidity fluctuations of velocity can be detected by hot wires only if their response frequency is higher than f_K.

Next we consider the local turbulence Reynolds number defined based on λ by $\mathrm{Re}_\lambda = \langle u^2\rangle^{1/2}\lambda/\nu$. Figure 10 shows the centerline variation of Re_λ. According to equation (25), in the self-preserving region, $\mathrm{Re}_\lambda = C_R\,\mathrm{Re}^{1/2}[(x-x_0)/d]^{1/4}$ for the plane jet ($\alpha = 2$), while $\mathrm{Re}_\lambda = C_R\,\mathrm{Re}^{1/2}$ for the circular jet ($\alpha = 1$). That is, the local turbulence Reynolds number of the two jets should behave quite differently in the far-field region: Re_λ is a constant in the circular jet but increases slowly with x in the form of $\mathrm{Re}_\lambda \propto x^{1/4}$. This is indeed verified in figure 10 by the results of Re_λ estimated from λ for $x/d > 10$. On the other hand, without use of the digital filter, not all the data follow (21)–(25) in the self-preserving region of both jets.

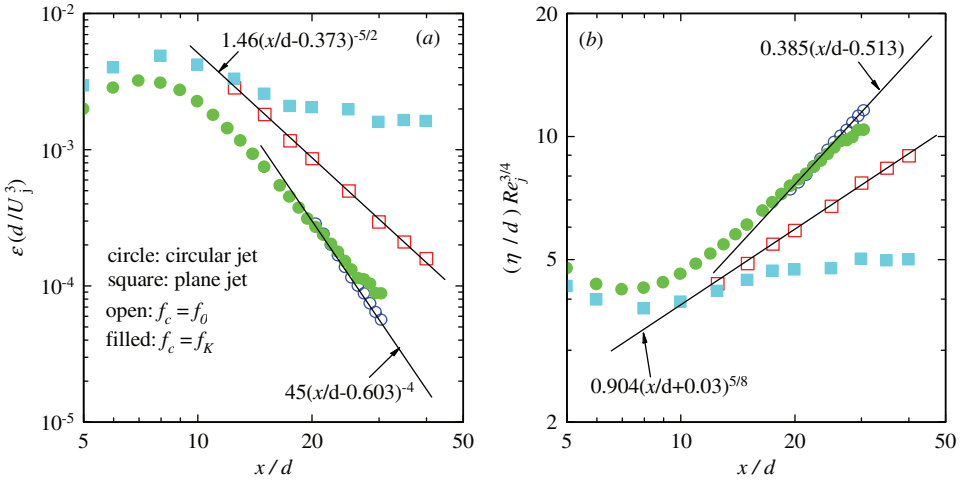

Figure 8. Centerline variations of (*a*) energy dissipation rate and (*b*) Kolmogorov scale.

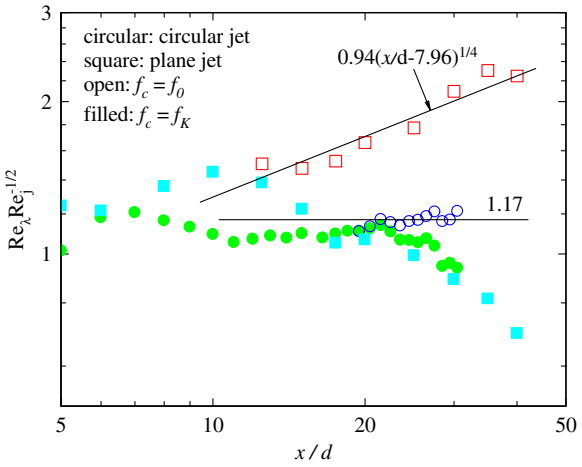

Figure 10. Centerline variation of the Taylor Reynolds number.

6. Concluding remarks

Based on definitions (2) and (3) for the Kolmogorov scales η and f_K, Mi *et al* [8] have developed a fast-convergent-iteration filtering scheme that not only removes the unwanted noise contribution from the measured signal of velocity (u_{im}) but also finds the 'true' values of λ, η and f_K without any arbitrariness. The scheme uses (7)–(9) circularly to 'squeeze out' the noise-error from u_{im} by filtering u_{im} at new f_{Km} iteratively. The principle is based on the fact that the noise has a significantly greater influence on ε_m than on both η_m and f_{Km}. The scheme has been well validated presently by analyzing the measured data of u_m against the self-preserving relations (21)–(25) whose validity has long been proven firmly by many independent experiments in the literature.

Accordingly, several conclusions on the digital filter scheme can be drawn below.

(1) The scheme is of important significance to enhance the basic research on fine-scale turbulence, because most studies to date have used hot-wire anemometry (e.g. [1, 7]). It is believed that many of the previously derived conclusions on fine-scale turbulence may suffer, to an unknown extent, from the contamination of high-frequency electronic noise.

(2) Application of this scheme will allow future hot-wire measurements to unambiguously determine the appropriate cut-off frequency, hence generating more reliable data for better understanding of fundamental small-scale turbulence.

(3) The scheme is much simpler and more rigorous than the electronic filter schemes adopted previously by, e.g., Antonia *et al* [4, 15], Champagne [5] and Bailey *et al* [7], for hot-wire measurements of small-scale turbulence properties.

(4) The use of the digital filter does not require any electronic filter and other relevant devices. Significantly, it has largely simplified the process of hot-wire measurements.

(5) The scheme should also be applied for achieving the reliable measurement of temperature (scalar) using a cold-wire anemometer, in which the Batchelor, instead of the Kolmogorov, scales may be found. Reliable data on a turbulent scalar will certainly help to better understand the fundamental turbulence.

(6) The noise effect is basically uncorrelated with the hot-wire length. So, the above conclusions still apply even when the wire length is too long to well resolve the smallest scales of turbulence.

Acknowledgments

The support of Nature Science Foundation of China through grants 10921202 and 11072005 is gratefully acknowledged. We thank Dr R C Deo for his centerline measurements of the instantaneous velocity in a plane jet, during his PhD study at the University of Adelaide. We are also indebted to all the anonymous referees for their insightful comments, the addressing of which has strengthened the paper significantly.

References

[1] Sreenivasan K R and Antonia R A 1997 The phenomenology of small-scale turbulence *Annu. Rev. Fluid Mech.* **29** 435–72
[2] Buch K and Dahm W 1998 Experimental study of the fine-scale structure of conserved scalar mixing in turbulent shear flows: part 2. Sc ∼1 *J. Fluid Mech.* **364** 1–29
[3] Su L and Clemens N 1999 Planar measurements of the full three-dimensional scalar dissipation rate in gas-phase turbulent flows *Exp. Fluids* **27** 507–21
[4] Antonia R A, Satyaprakash B R and Hussain A 1980 Measurements of dissipation rate and some other characteristics of turbulent plane and circular jets *Phys. Fluids* **23** 695–700
[5] Champagne F 1978 The fine-scale structure of the turbulent velocity field *J. Fluid Mech.* **86** 67–108
[6] Cai J and Tong C 2009 A conditional sampling-based method for noise and resolution corrections for scalar dissipation rate measurements *Phys. Fluids* **21** 065104
[7] Bailey S, Hultmark M, Schumacher J, Yakhot V and Smits A 2009 Measurement of local dissipation scales in turbulent pipe flow *Phys. Rev. Lett.* **103** 14502
[8] Mi J, Deo R C and Nathan G J 2005 Fast-convergent iterative scheme for filtering velocity signals and finding Kolmogorov scales *Phys. Rev.* E **71** 066304
[9] Antonia R A and Mi J 1993 Temperature dissipation in a turbulent round jet *J. Fluid Mech.* **250** 531–51
[10] Mi J and Nathan G J 2003 The influence of probe resolution on the measurement of a passive scalar and its derivatives *Exp. Fluids* **34** 687–96
[11] Wang G, Clemens N, Barlow R and Varghese P 2007 A system model for assessing scalar dissipation measurement accuracy in turbulent flows *Meas. Sci. Technol.* **18** 1287–303
[12] Hinze J O 1975 *Turbulence: An Introduction to its Mechanism and Theory* (New York: McGraw-Hill)
[13] Kuo A Y-S and Corrsin S 1971 Experiments on internal intermittency and fine-structure distribution functions in fully turbulent fluid *J. Fluid Mech.* **50** 285–319
[14] Frenkiel F, Klebanoff P and Huang T 1979 Grid turbulence in air and water *Phys. Fluids* **22** 1606
[15] Antonia R A, Satyaprakash B and Hussain A 1982 Statistics of fine-scale velocity in turbulent plane and circular jets *J. Fluid Mech.* **119** 55–89
[16] Deo R C, Mi J and Nathan G J 2007 The influence of nozzle aspect ratio on plane jets *Exp. Therm. Fluid Sci.* **31** 825–38
[17] Mi J, Xu M and Du C 2011 Reynolds number influence on turbulent mixing characteristics of a circular free jet *Exp. Fluids* submitted

[18] Champagne F H, Sleicher C A and Wehrmann O H 1967 Turbulence measurements with inclined hot wires: part 1. Heat transfer experiments with inclined hot wire *J. Fluid Mech.* **28** 153–75
[19] Mi J and Antonia R A 1994 Corrections to Taylor hypothesis in a turbulent circular jet *Phys. Fluids* **6** 1548–52
[20] Wyngaard J and Clifford S 1977 Taylor's hypothesis and high-frequency turbulence spectra *J. Atmos. Sci.* **34** 922–9
[21] Antonia R A, Phan-Thien N and Chambers A J 1980 Taylor's hypothesis and the probability density functions of temporal velocity and temperature derivatives in a turbulent flow *J. Fluid Mech.* **100** 193–208
[22] Lele S 1992 Compact finite difference schemes with spectral-like resolution *J. Comput. Phys.* **103** 16–42
[23] Mi J and Antonia R 2010 Approach to local axisymmetry in a turbulent cylinder wake *Exp. Fluids* **48** 933–47
[24] Tennekes H and Lumley J 1972 *A First Course in Turbulence* (Cambridge, MA: MIT Press)
[25] Gutmark E and Wygnanski I 1976 The planar turbulent jet *J. Fluid Mech.* **73** 465–95
[26] Deo R C, Mi J and Nathan G J 2007 The influence of nozzle-exit geometric profile on statistical properties of a turbulent plane jet *Exp. Therm. Fluid Sci.* **32** 545–59